

Proceeding Paper

Weak Donor, Strong Acceptor Thienopyrazine-Based Polymers for Fine Tuning of LUMO Levels—Suitable Materials for Energy and Storage Solutions [†]

Benedetta Maria Squeo ^{1,*}, Elisa Lassi ¹, Chiara Botta ¹, Silvia Luzzati ¹, Barbara Vercelli ², Stefania Zappia ¹ and Mariacecilia Pasini ^{1,*}

¹ Istituto di Scienza e Tecnologie Chimiche (SCITEC), Consiglio Nazionale Delle Ricerche, Via Corti 12, 20133 Milano, Italy; lassi@ismac.cnr.it (E.L.); chiara.botta@scitec.cnr.it (C.B.); silvia.luzzati@scitec.cnr.it (S.L.); stefania.zappia@scitec.cnr.it (S.Z.)

² Istituto di Chimica Della Materia Condensata e di Tecnologie per l'Energia (ICMATE), Consiglio Nazionale Delle Ricerche, Via Roberto Cozzi 53, 20125 Milano, Italy; barbara.vercelli@cnr.it

* Correspondence: benedetta.squeo@scitec.cnr.it (B.M.S.); mariacecilia.pasini@scitec.cnr.it (M.P.)

[†] Presented at the 25th International Electronic Conference on Synthetic Organic Chemistry, 15–30 November 2021; Available online: <https://ecsoc-25.sciforum.net/>.

Abstract: One approach creating and to tuning the energy levels of small band gap polymers or molecules is alternating donor-like (electron donating) and acceptor-like (electron withdrawing) monomers. Polymer for solar cells need to maintain a low highest occupied molecular orbital (HOMO) energy level in order to maximize the open circuit voltage (V_{oc}) and have a small band gap in order to maximize the short-circuit current (J_{sh}). Alternating a “weak donor” and a “strong acceptor” will maintain a low HOMO energy level and reduce the band gap via intramolecular charge transfer (ICT). Here we present the synthesis and characterization of a series of polymers based on thienopyrazine (acceptor) and carbazole (donor). We compared the optoelectronic properties of the classic polymer poly-carbazole-dithiophene-benzothiadiazole (PCDTBT) with one where benzothiadiazole was substituted with thienopyrazine and one where we randomly alternated thienopyrazine and benzothiadiazole as the acceptor unit while maintaining the same donor unit. The approach of alternating weak donor and strong acceptor moieties allowed us to obtain fine LUMO level modulation of the materials, opening the way to the design of new donor materials.

Keywords: low band-gap polymers; OPVs; semiconducting polymers; thienopyrazine



Citation: Squeo, B.M.; Lassi, E.; Botta, C.; Luzzati, S.; Vercelli, B.; Zappia, S.; Pasini, M. Weak Donor, Strong Acceptor Thienopyrazine-Based Polymers for Fine Tuning of LUMO Levels—Suitable Materials for Energy and Storage Solutions. *Chem. Proc.* **2022**, *8*, 71. <https://doi.org/10.3390/ecsoc-25-11742>

Academic Editor: Julio A. A. Seijas Vázquez

Published: 14 November 2021

Publisher's Note: MDPI stays neutral with regard to jurisdictional claims in published maps and institutional affiliations.



Copyright: © 2021 by the authors. Licensee MDPI, Basel, Switzerland. This article is an open access article distributed under the terms and conditions of the Creative Commons Attribution (CC BY) license (<https://creativecommons.org/licenses/by/4.0/>).

1. Introduction

The increasing global energy demand and the necessity to shift from fossil fuels to renewable energy sources demand changes in energy production and storage solutions.

Conjugated semiconducting materials in between conjugated polymers may be the protagonists of this epochal change of paradigm because they can be low-cost, lightweight, flexible, derived from abundant raw materials, low in toxicity, low in environmental impact and able to meet to circular chemistry demands [1–7].

Additionally, a wide range of electronic properties can be accessed through well-developed synthetic organic chemistry. This has allowed conjugated polymers to provide optical and electronic properties for many applications, such as light-emitting diodes (OLEDs), organic photovoltaics (OPVs), field-effect transistors (OFETs), biosensors and energy storage devices [8–15].

As far as p-type materials are concerned, satisfactory results have already been obtained, but there is still much to be done with n-type materials [16–18]. The development of new n-type materials is fundamental for the creation of organic solar cells with efficiencies exceeding 10%, but it is also particularly significant for pseudocapacitors based on conjugated polymers [19]. In fact, most of these conjugated polymers are only capable of storing

charge in a “positive” potential range, which results in low operating voltages and limited energy and power densities due to the lack of stable n-type redox-active materials [20].

The D–A approach with the repeating units consisting of an electron-donating (donor) moiety and an electron-withdrawing (acceptor) moiety has been successfully proposed for developing this class of materials [21–24]; specifically, donor–acceptor copolymers are combinations of an electron donor and an acceptor unit copolymerized via traditional organometallic coupling [25]. As shown in Figure 1, hybridization of frontier molecular orbitals (HOMO and LUMO) of donor and acceptor units yields a low bandgap material with absorption extended into the near-IR region, which has made these systems popular in OPVs’ active layers. Moreover, polymers for solar cells need to maintain a low HOMO energy level in order to maximize the open circuit voltage (V_{oc}), and a small band gap in order to maximize the short-circuit current (J_{sh}) [26–28]: alternating a “weak” donor and a “strong” acceptor will maintain a low HOMO energy level thanks to the weak donor, and reduce the band gap via Intramolecular charge transfer (ICT) thanks to the “strong” acceptor [29,30].

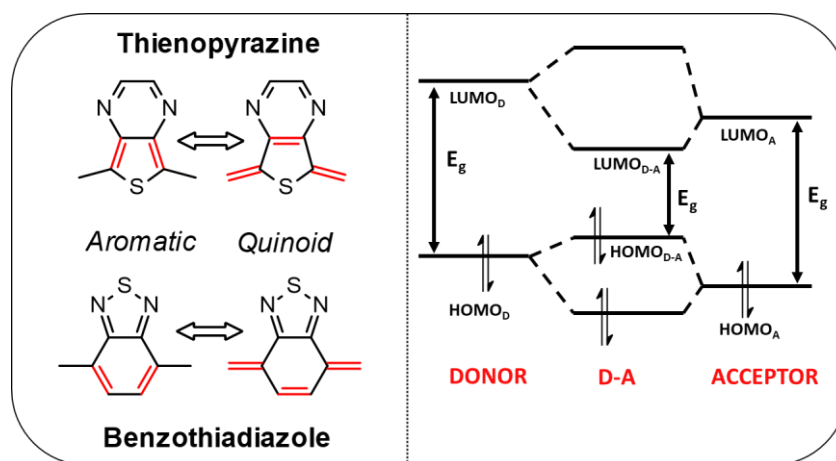


Figure 1. Aromatic and quinoid resonance structures of thienopyrazine and benzothiadiazole units (left). Hybridization of frontier molecular orbitals (HOMO and LUMO) of donor and acceptor units (right).

Very recently [31], the use of the proquinoidal acceptors strategy has been proposed for the development of n-type copolymers, as it is able to promote strong π -electron correlations, extensive delocalization and a very narrow bandgap. An aromatic moiety can in fact be described as “proquinoidal” if it has an important resonance contribution from the quinoidal form, and the proquinoidal character can be improved by fusing additional aromatic rings [32]. Notable examples of proquinoidal–aromatic copolymers with proquinoidal building blocks, including thieno[3,4-*b*]pyrazine (TP) [33], have been developed as active materials for organic field-effect transistors, photovoltaics, organic light-emitting diodes and many other applications [34].

The TP structure is an isomer of the well-known 2,1,3-benzothiadiazole (BT) [35], which has been successfully employed as an OPV active material, achieving PCEs over 18% [36,37]. In addition, the TP unit, unlike BT (Figure 1), has an important resonance contribution from the quinoidal form in the resonance structures, forming a six membered aromatic sextet, and thus additionally lowering the band gap of conjugated polymers with respect to BT [38]. Another potential advantage of TP in conjugated polymers is that the TP moiety provides a more planar backbone between repeating units owing to decreased steric hindrance of the thiophene ring compared to the benzene ring in BT-based copolymers.

TP-based materials have been developed for OPV applications, and moreover, they possess many attributes that are advantageous to pseudo-capacitors, such as the ability to reversibly store negative charge [19,39].

By miming the well-known poly[N-9'-heptadecanyl-2,7-carbazole-alt-5,5-(4',7'-di-2-thienyl-2',1',3'-benzothiadiazole)] (PCDTBT), we have synthesized the analogue poly[N-9'-heptadecanyl-2,7-carbazole-alt-5,5-(4',7'-di-2-thienyl-2-thieno[3,4-e]pyrazines)] and a random copolymer 9-(9-Heptadecanyl)-9H-carbazole-2,7-diboronic acid bis(pinacol) ester containing 4,7-Bis(2-bromo-5-thienyl)-2,1,3-benzothiadiazole and 4,7-Bis(2-bromo-5-thienyl)-2 Thieno[3,4-e]pyrazines). In our polymers, there is significant internal charge transfer character between electron-rich (donor) and electron-deficient (acceptor) components; furthermore, they maintain the ability to reversibly store negative charge, and the random copolymer approaches [40] seem to be effective for the fine modulation of HOMO and LUMO levels. Finally, the polymers are highly soluble in organic solvents and can be processed by solution deposition approaches, rendering them versatile and scalable.

2. Materials and Methods

General Information for synthesis. Unless specifically mentioned, all reagents were purchased from a commercial source and used without further purification. Toluene was freshly distilled prior to use according to a procedure in the literature. All reactions were carried out in inert atmosphere. Compound M1 was prepared according to the procedures reported in the literature [41,42].

PCDTBT was purchased from 1-Materials. PC₇₀BM (99.5% purity) was purchased from Solenne BV.

Electrochemistry. Electrochemistry was performed at room temperature in acetonitrile under nitrogen in three electrode cells. The counter electrode was platinum; reference electrode was Ag/Ag⁺ (0.1 m AgNO₃ in acetonitrile, 0.34 V vs. SCE, −4.73 V vs. vacuum); supporting electrolyte was 0.1 m tetrabutylammonium perchlorate (TBAP). The voltammetric apparatus was Metrohm Autolab 128N potentiostat/galvanostat. The working electrode for cyclic voltammetry (CV) was a glassy-carbon (CG) minidisc electrode (0.2 cm²). HOMO and LUMO levels were estimated according to the equation $E_{\text{HOMO}} = -(E_{\text{ox}} + 4.39 + 0.34)$ [43]. PCDTBT, PCDTTB and PC(DTTP)₅(DTBT)_{0.5} films were casted on a preheated electrode surface at around 60 °C. By means of a micro-syringe, 2 μL of 2 mg mL^{−1} chloroform solutions of the polymers were dropped on the electrode surface.

Size Exclusion Chromatography (SEC). The molecular weight distribution (MWD) of every sample was obtained by an integrated high-temperature (HT) size exclusion chromatography (SEC) system. The chromatographic system consisted of a GPCV2000 system from Waters (USA) equipped on-line with a differential refractometer (DRI) as concentration detector.

Experimental Conditions: column set constituted a 3 Shodex HT from Showa Denko (Japan); mobile phase: o-dichlorobenzene (o-DCB); flow rate: 0.8 mL/min; temperature: 135 °C.

Nuclear Magnetic Resonance (NMR). ¹H NMR and ¹³C NMR spectra were recorded with a Bruker DRX 600 MHz spectrometer.

Synthesis of compound M2. Compound M1 (140 mg, 0.47 mmol, 1 eq.) was dissolved in dry chloroform (CHCl₃, 25 mL) and cooled down to 0 °C. Then, N-bromosuccinimide (NBS; 174 mg, 0.98 mmol, 2.1 eq.) and glacial acetic acid (CH₃COOH, 25 mL) were added. The reaction was allowed to reach room temperature in the dark by shielding the flask with aluminum foil. After 1 h at room temperature, the crude product was diluted with CHCl₃ and washed 3 times with a saturated sodium bicarbonate (NaHCO₃) solution. The organic solvent was removed under reduced pressure, and the product was purified by silica gel chromatography and recrystallized from hexane/dichloromethane (143 mg, 66% yield). ¹H NMR (CDCl₃) δ (ppm): 8.51 (s, 2H), 7.31 (d, 2H), 7.1(d, 2H).

Synthesis of polymer PCDTTP. A mixture of monomer M2(65 mg, 0.142 mmol, 1 eq.), 9-(9-heptadecanyl)-9H-carbazole-2,7-diboronic acid bis(pinacol) ester (93 mg, 0.142 mmol, 1 eq.), Tetrakis(triphenylphosphine)palladium(0) (Pd(PPh₃)₄) (3.3 mg, 2% mmol) and tetrabutylammonium bromide (TEBAB) was added to a predegassed schlenk, followed by three vacuum/nitrogen cycles. Then, dry toluene (4 mL) and degassed potassium

carbonate aqueous (2 mL) solution were added. The mixture was stirred at 110 °C. After 5 h, there was precipitation of the polymer, and the reaction was quenched. The crude was precipitated in methanol. The polymer was washed on Soxhlet apparatus with methanol, hexane and chloroform. The chloroform fraction was evaporated under reduced pressure, and the polymer was precipitated in methanol, filtered and dried under high vacuum, providing a dark solid (25 mg, 35% yield of chloroform fraction). $^1\text{H NMR}$ (CDCl_3) δ (ppm): 8.6 (broad, 2H), 8.1–8.0 (broad, 2H), 7.9–7.7 (broad, 4H), 7.58 (broad, 2H), 7.4 (broad, 2H), 4.1 (broad, 1H) 1.2–1.1 (broad, 26H), 0.8 (broad, 8H); MW = 3.7 kDa, MN = 8.1 kDa, PD = 2.22.

Synthesis of polymer PC(DTTP)_{0.5}(DTBT)_{0.5}. A mixture of monomer M2 (58 mg, 0.126 mmol, 0.5 eq.), 4,7-Bis(5-bromo-2-thienyl)-2,1,3-benzothiadiazole (58 mg, 0.126 mmol, 0.5 eq.), 9-(9-heptadecanyl)-9H-carbazole-2,7-diboronic acid bis(pinacol) ester (166 mg, 0.253 mmol, 1 eq.), Tetrakis(triphenylphosphine)palladium(0) ($\text{Pd}(\text{PPh}_3)_4$) (6 mg, 2% mol) and tetrabutylammonium bromide (TEBAB) was added to a predegassed schlenk, followed by three vacuum/nitrogen cycles. Then, dry toluene (6 mL) and degassed potassium carbonate aqueous solution (3 mL) were added. The mixture was stirred at 110 °C. After 6 h, the polymer started to precipitate, and the reaction was quenched. The crude was precipitated in methanol. The polymer was washed on Soxhlet apparatus with methanol, hexane and chloroform. The chloroform fraction was evaporated under reduced pressure, and the polymer was precipitated in methanol, filtered and dried under high vacuum, providing a dark solid (95 mg, 46% yield of chloroform fraction). $^1\text{H NMR}$ (CDCl_3) δ (ppm): 8.54 (broad, 2H), 8.2–8.1 (broad, 4H), 7.9–7.7 (broad, 6H), 7.6–7.4 (broad, 4H), 7.2–7.0 (broad, 2H), 4.8–4.7 (broad, 1H) 1.2–1.1 (broad, 26 H), 0.8 (broad, 8H). (MW = 3.2 kDa, MN = 6.1 kDa, PD = 1.81).

Device Fabrication and Photovoltaic Characterization

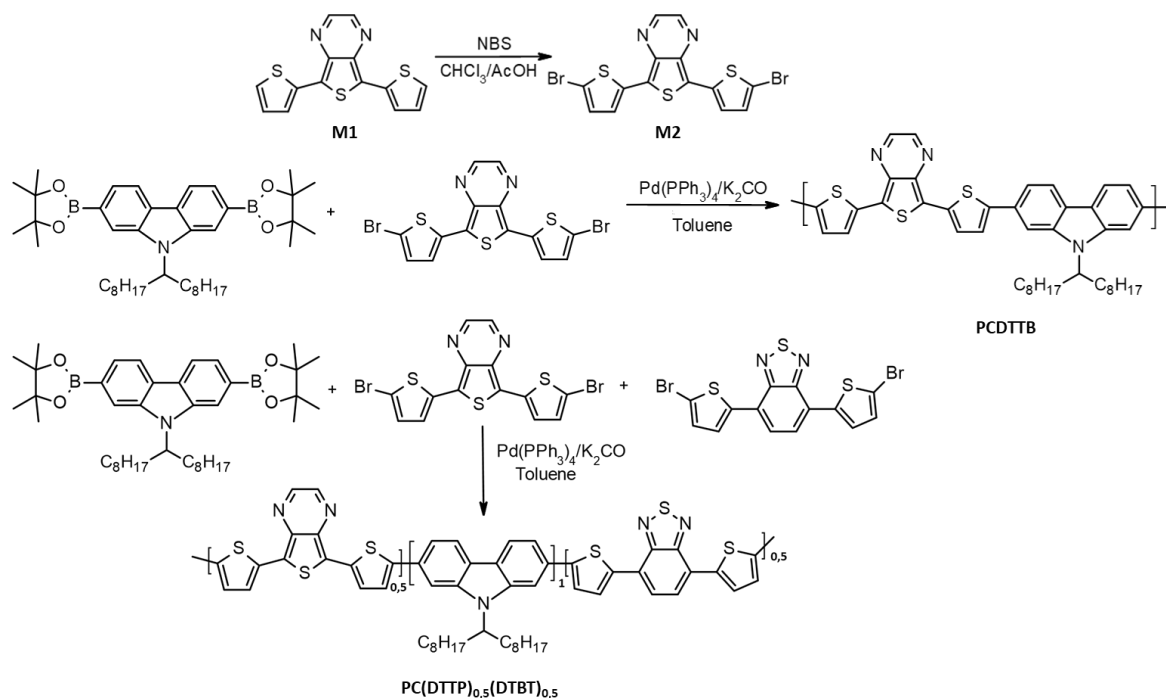
Direct Geometry devices' fabrication. Solar cells were assembled with the conventional structure: glass/ITO/PEDOT:PSS/PCDTTP:PC₇₀BM/Ca/Al. Glass ITO (Kintec) 15 Ω /sq substrates were mechanically cleaned with peeling tape and paper with acetone and then were washed in a sonic bath at 50 °C for 10 min sequentially with water, acetone and isopropanol. After drying with compressed nitrogen flow, 10 min plasma treatment in the air was used to enhance ITO wettability for the next deposition. PEDOT:PSS (Al VP 8030 from Heraus) was filtered on a 0.45 μm nylon filter and spin-coated in the air at 2500 rpm for 50 s. The device assembly was then performed in a glovebox. The active layer was composed by a blend dissolved at 1:4 wt/wt of PCDTTP:PC₇₀BM solution in a 1,2-dichlorobenzene–chlorobenzene 3:1 *v:v* mixture at a total concentration of 30 mg/mL. The solution was stirred for 12 h on a hotplate in glovebox at 60 °C. The active layer was spin-coated from the warm solution at 1000 rpm for 60 s, which resulted in a thickness of 95 nm; at 1200 rpm for 60 s, which resulted in a thickness of 85; and at 1500 rpm for 60 s, which resulted in a thickness of 70 nm. Finally, the substrates were stored in a glovebox and annealed at 70 °C for 15 min. Finally, 10 nm of calcium and a 100 nm thick aluminum electrode were evaporated on the top of the device through a shadow mask under a pressure of 2×10^{-6} mbar. The deposition rate was 0.5 nm/s. There were six devices on a single substrate, each with an active area of 6.1 mm².

Device characterization and measurements. The devices were characterized through current density–voltage and external quantum efficiency characterization. Current density–voltage measurements were performed directly in the glovebox where the solar cells were assembled, with a Keithley 2602 source meter, under an AM 1.5G solar simulator (ABET 2000). The incident power, measured with a calibrated photodiode (Si cell + KG5 filter), was 100 mW/cm². The EQE spectral responses were recorded by dispersing an Xe lamp through a monochromator, using an Si solar cell with a calibrated spectral response to measure the incident light power intensity at each wavelength. The devices were taken outside the glovebox for the EQE measurements, after mounting them on a sealed cell to avoid moisture and oxygen exposure.

3. Results and Discussion

3.1. Chemical Characterization

Polymers PCDTTP and PC(DTTP)_{0.5}(DTBT)_{0.5} were synthesized through Suzuki cross-coupling of a dibromide of the acceptor units and the bis-boronic ester of carbazole, with Pd(PPh₃)₄ as a catalyst and K₂CO₃ as a base in degassed toluene as solvent (Scheme 1). Both polymers showed low molecular weight due to the poor solubility of the growing chain during polymerization.



Scheme 1. Synthesis of compound M2, polymer PCDTTP and polymer PC(DTTP)_{0.5}(DTBT)_{0.5}.

The yields of the polymers were 35% for PCDTTP and 46% PC(DTTP)_{0.5}(DTBT)_{0.5} and were calculated for only the chloroform soluble fraction. As reported in the literature, randomly distributed conjugated terpolymers may have higher solubility and a lower tendency to aggregate in comparison to their parent polymers with more regularly repeating units [44]. Additionally, in this case the different yields was most probably due to the lower solubility of PCDTTP with respect to PC(DTTP)_{0.5}(DTBT)_{0.5}. After the extraction in chloroform, there was still some PCDTTP that was not soluble even in dichlorobenzene.

We decided to use a non-substituted TP derivative in order to have a direct comparison with the well-known PCDTBT copolymer. Moreover, the strategy of donor–acceptor conjugated polymers with minimally substituted acceptor moieties [45] has been revealed to be particularly useful in order to understand the electronic role of the acceptor, and the impact of the steric hindrance of the acceptor can be clarified in future studies by inserting linear or branched lateral alkyl chains into TP, or thienyl moieties. For this reason, it was not possible to use palladium-catalyzed direct C–H arylation coupling due to the formation of cross-linked byproducts in the unsubstituted positions [46].

The ¹H NMR spectra of the two synthesized polymers confirmed the presence of the polymers. The peaks are large and broad, in line with the polydispersity and poor solubility of the materials in room temperature CDCl₃. The FT-IR spectra showed the characteristic aliphatic and aromatic C–H bending between 3000 and 2700 cm^{−1}, and the C=C and C=N stretching that is characteristic of aromatic compounds.

3.2. Optoelectronic Characterization

The absorption spectra in thin films and CHCl₃ solution of the synthesized polymers PCDTTP and PC(DTTP)_{0.5}(DTBT)_{0.5} and the purchased PCDTB were recorded. The polymers showed two major absorption peaks, a common feature for alternating D–A copolymers, and the two new polymers showed red-shifted absorption compared to PCDTBT. In particular, the random copolymer PC(DTTP)_{0.5}(DTBT)_{0.5} showed a panchromatic absorption spectrum from 450 to 700 nm (Figure 2), and the low energy peak, ascribed to intramolecular charge transfer (ICT), showed the two contributions of the precursor copolymers.

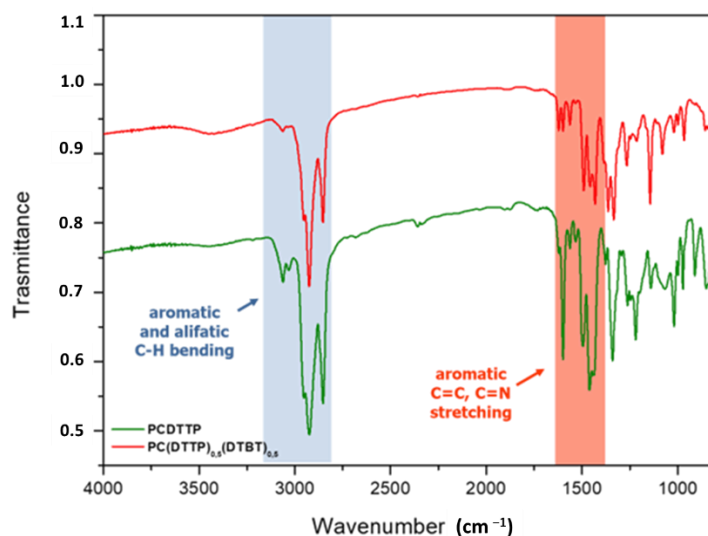


Figure 2. FT-IR spectra of polymers PCDTTP and PC(DTTP)_{0.5}(DTBT)_{0.5}.

The optical energy gap (Table 1) was calculated from the onset of the solid-state absorption spectra: the two new polymers have roughly the same energy gap (1.60 eV), smaller than that of the PCDTB polymer (1.89 eV).

Table 1. Optoelectronic properties of polymers PCDTBT, PCDTTP, PC(DTTP)_{0.5}(DTBT)_{0.5}.

Polymer	Solution [nm] ^a		Film [nm] ^b		E _g ^{opt} [eV] ^c	E _{ox} [eV]	E _{red} [eV]	HOMO [eV] ^d	LUMO [eV]	E _g ^{cv} [eV] ^e
	λ _{max}		λ _{max}	λ _{onset}						
PCDTBT	560		581	656	1.89	0.53	−1.70	−5.27	−3.03	2.24
PCDTTP	635		655	775	1.61	0.35	−1.56	−5.08	−3.17	1.91
PC(DTTP) _{0.5} (DTBT) _{0.5}	518; 611		550; 640	766	1.60	0.20	−1.51	−4.93	−3.23	1.7

^a Diluted polymer solution in CHCl₃; ^b thin film on glass; ^c estimated from the absorption band edge in the film, E_g^{opt} = 1240/λ_{onset} (eV); ^d E_{HOMO} = −4.39 − (E_{ox} + 0.34) eV; E_{LUMO} = −4.39 − (E_{red} + 0.34) eV; ^e E_g^{cv} = E_{LUMO} − E_{HOMO}.

Cyclic voltammetry (CV) determinations (Figure 3b) showed that PCDTBT and PCDTTP presented one irreversible oxidation process each, at 0.589 and 0.627 V, respectively, which probably involves their electron-donating (donor) moieties. In PC(DTTP)_{0.5}(DTBT)_{0.5}, the oxidation process split into two reversible ones separated by ca. 0.24 V (see Table 1). The latter could be a solid-state effect which may be accounted for by the formation of mixed-valence states analogous to those found in TTF polymers [47]. All samples presented a single reversible reduction process, at comparable potentials, which is probably localized on the electron-withdrawing (acceptor) moieties of the molecules.

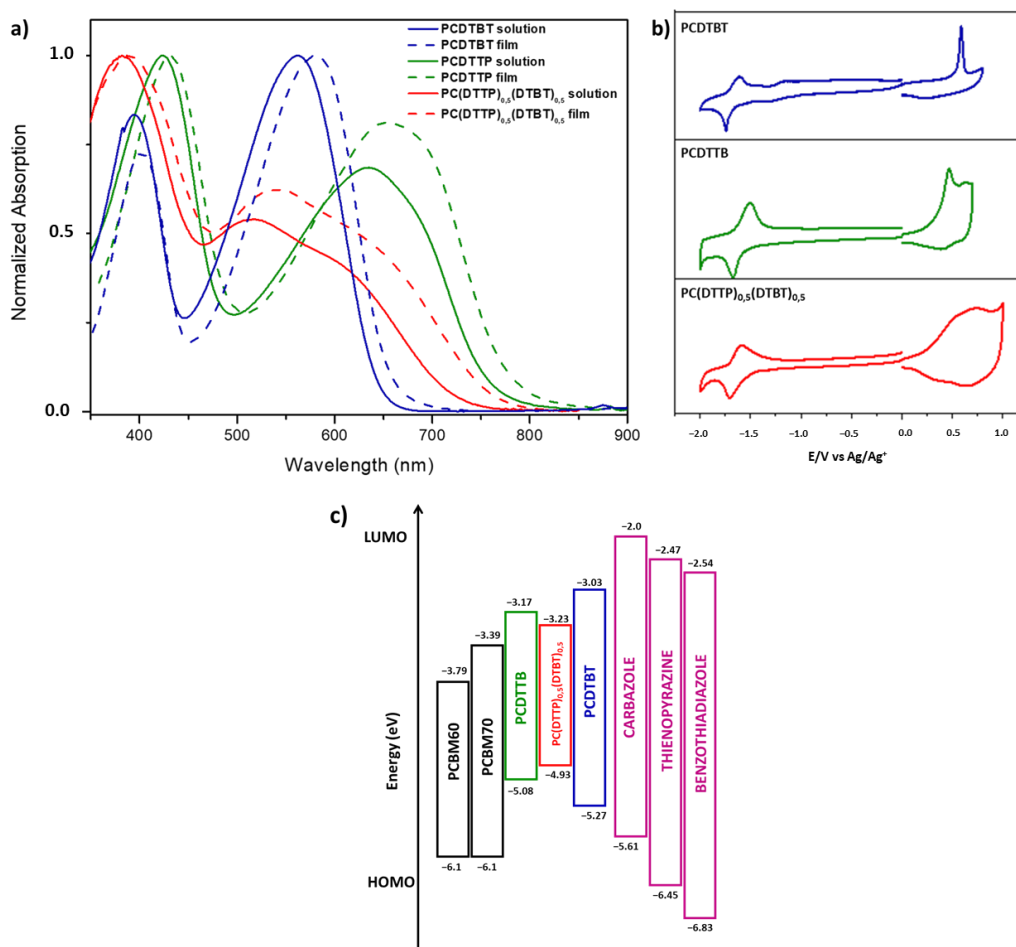


Figure 3. (a) Absorption spectra in an CHCl_3 solution and in a solid state for polymers PCDTBT, PCDTTP, $\text{PC(DTTP)}_{0.5}(\text{DTBT})_{0.5}$. (b) Voltammograms of polymers PCDTBT, PCDTTP, $\text{PC(DTTP)}_{0.5}(\text{DTBT})_{0.5}$. (c) Energy levels diagram.

It is important to underline a lowering of the electrochemical E_g from PCDTBT to PCDTTP, and then to $\text{PC(DTTP)}_{0.5}(\text{DTBT})_{0.5}$. This behavior can be attributed to the greater contribution of the quinoid form in the polymer containing the TP unit additionally lowering the band gap. Furthermore, the presence of the TP moiety resulted in increased backbone planarity thanks to the decreased steric hindrance of the five membered thiophenic ring compared to the six membered benzenic ring. The further decrease in electrochemical E_g in the random copolymer can be attributed to the increase in the mean length of conjugation in the D–A segments.

We have investigated the influences of the solvent polarity on the optical properties of the polymers PCDTTP and $\text{PC(DTTP)}_{0.5}(\text{DTBT})_{0.5}$, as shown in Figure 4. We have analyzed absorption and emission spectra in six different solvents, and we observed that absorption spectra were poorly influenced by the polarity of the solvent. In the emission spectra, we observed solvatochromism. The emission spectra of the polymers were redshifted with increasing solvent polarity. To confirm, we plotted the redshift vs. solvent polarity: in Figure 4e, a clear linear correlation can be observed, which is ascribed to the stabilization of the highly polar, excited charge-transfer states in more polar solvents, typical of donor–acceptor emitters [48,49].

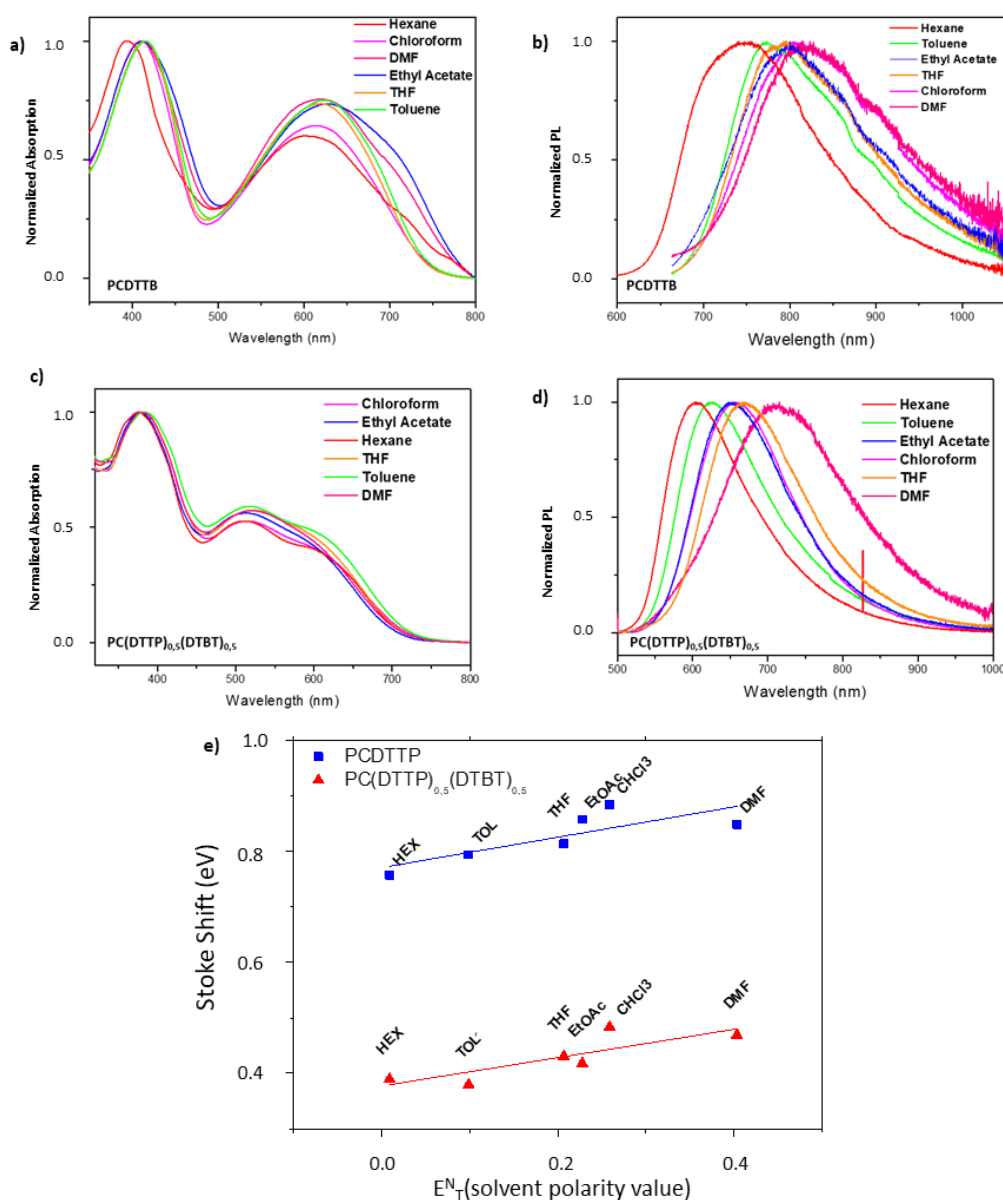


Figure 4. Absorption and emission spectra of polymers PCDTTP (a,b) and PC(DTTP)_{0.5}(DTBT)_{0.5} (c,d) in different solvents (hexane, toluene, chloroform, tetrahydrofuran, N,N-dimethylformamide, ethyl acetate). (e) Stokes shifts (solid points) against normalized solvent polarity parameter E_T^N with the best linear fit (solid lines).

3.3. Photovoltaic Characterization

The photovoltaic characteristics were investigated upon blending PCDTTP with PC₇₁BM in bulk heterojunction devices. The current density–voltage curves (J–V) of devices with different active layer thicknesses under AM1.5-simulated solar light illumination (100 mW/cm²) are shown in Figure 5a, and the corresponding photovoltaic parameters are depicted in Table 2. The power conversion efficiency (η) obtained with PCDTTP reached 1.24%, which is in line to the values reported in the literature for other TP-based OPV devices [39]. The PCDTTP devices exhibited an open circuit voltage (V_{oc}) of 0.58 V, which is about 0.2–0.3 V lower than the benchmark PCDTBT solar cells according to the literature [50]. Such a reduction in the V_{oc} could result from the upward shift of the HOMO level of PCDTTP, as displayed in Figure 3c [26]. In addition, the short-circuit current density J_{sc} reached 5.5 mA/cm² in PCDTTP devices, which is about a half of the typical values reported for benchmark PCDTBT cells [49]. One of the reasons that may eventually contribute

to the relatively lower J_{sc} and EQE values is the lower LUMO-energy-level offset between the polymer and the fullerene component, which may limit the charge photogeneration yield [51]. The relatively low FF of 0.39 suggests non-optimal charge separation or transport to the electrodes. Interestingly, the EQE spectrum displayed in Figure 5b exhibits an onset at 780 nm (1.59 eV), which is red-shifted when compared to PCDTBT devices [52]. This is consistent with the reduced optical energy gap of PCDTTP displayed in Table 1.

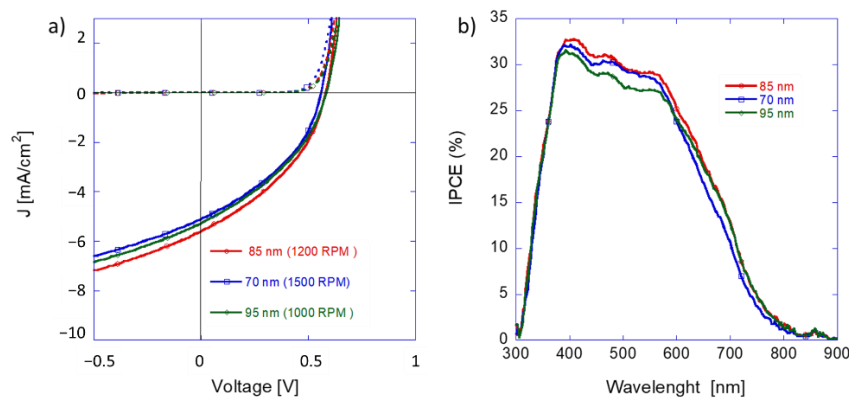


Figure 5. (a) Current density–voltage curves vs. active layer thicknesses of PCDTTP:PC71BM devices. Continuous lines: under 1 sun of AM1.5G solar simulation (100 mW/cm²); dotted lines: dark curves. (b) EQE spectra vs. active layer thicknesses of PCDTTP:PC71BM devices.

Table 2. Summary of the photovoltaic parameters.

Thickness	V_{oc} [V]	FF [-]	J_{sc} [mAcm ⁻²]	η [-]	J_{sc}^{EQE} [mAcm ⁻²] ^a
70	1.89	0.53	−5.27	−3.03	2.24
75	1.61	0.35	−5.08	−3.17	1.91
95	1.60	0.20	−4.93	−3.23	1.7

^a Calculated from the AM1.5G and EQE spectra.

4. Conclusions

In summary, we synthesized an alternating donor–acceptor copolymer via Suzuki coupling based on 9′-heptadecanyl-2,7-carbazole as the donor and 2-thienyl-2 thieno[3,4-e]pyrazines as the acceptor; the random terpolymer from the same donor unit; and two different acceptors unit—namely, 2-thienyl-2 thieno[3,4-e]pyrazine and its isomer, 2-thienyl-2′,1′,3′-benzothiadiazole. The polymers were chemically characterized; and their optical, electrochemical and photovoltaic properties were discussed also in comparison to the well-known PCDTBT.

The TP-based copolymer showed red-shifted absorption and emission spectra both in solution and as a thin film with respect to the isomeric-BT-based copolymer, likely due to the greater contribution of the quinoid form in the presence of TP. The random terpolymer showed extended absorption and lower electrochemical E_g compared to the parent polymers, and this behavior could be ascribed to the increased delocalization of the system due to the presence of two acceptors with different strengths, as previously observed [40].

This work will help guide the synthetic design of n-type materials that can be applied as acceptors in OPV devices, but also will contribute to the long-standing challenge of finding a stable n-type material for supercapacitors for energy storage. Specifically, we showed that it is possible to lower the LUMO levels by using random tercopolymer approaches with two different acceptor units while maintaining the electrochemical reversibility of the reduction.

Author Contributions: B.M.S. performed the synthesis of materials; E.L. contributed to OPV preparation and characterization; C.B. was responsible for PL spectra; S.L. contributed to the discussion of PV results; B.V. was responsible for CV; S.Z. was responsible for SEC and FT-IR characterization; M.P. and B.M.S. designed the study, discussed the data and prepared the manuscript. All authors have read and agreed to the published version of the manuscript.

Funding: This project has received funding from the ATTRACT-POSEIDON project funded by the EC under Grant Agreement 777222.

Institutional Review Board Statement: Not applicable.

Informed Consent Statement: Not applicable.

Data Availability Statement: Not applicable.

Conflicts of Interest: The authors declare no conflict of interest.

References

1. Lee, J.; Park, S.A.; Ryu, S.U.; Chung, D.; Park, T.; Son, S.Y. Green-Solvent-Processable Organic Semiconductors and Future Directions for Advanced Organic Electronics. *J. Mater. Chem. A* **2020**, *8*, 21455–21473. [[CrossRef](#)]
2. Di Mauro, E.; Rho, D.; Santato, C. Biodegradation of Bio-Sourced and Synthetic Organic Electronic Materials towards Green Organic Electronics. *Nat. Commun.* **2021**, *12*, 3167. [[CrossRef](#)] [[PubMed](#)]
3. Irimia-Vladu, M.; Głowacki, E.D.; Voss, G.; Bauer, S.; Sariciftci, N.S. Green and Biodegradable Electronics. *Mater. Today* **2012**, *15*, 340–346. [[CrossRef](#)]
4. Giraud, L.; Grelier, S.; Grau, E.; Hadziioannou, G.; Brochon, C.; Cramail, H.; Cloutet, E. Upgrading the Chemistry of π -Conjugated Polymers toward More Sustainable Materials. *J. Mater. Chem. C* **2020**, *8*, 9792–9810. [[CrossRef](#)]
5. Giovanella, U.; Pasini, M.; Botta, C. Organic Light-Emitting Diodes (OLEDs): Working Principles and Device Technology. In *Applied Photochemistry: When Light Meets Molecules*; Bergamini, G., Silvi, S., Eds.; Lecture Notes in Chemistry; Springer International Publishing: Cham, Switzerland, 2016; pp. 145–196. ISBN 978-3-319-31671-0.
6. Botta, C.; Betti, P.; Pasini, M. Organic Nanostructured Host–Guest Materials for Luminescent Solar Concentrators. *J. Mater. Chem. A* **2012**, *1*, 510–514. [[CrossRef](#)]
7. Lagonegro, P.; Giovanella, U.; Pasini, M. Carbon Dots as a Sustainable New Platform for Organic Light Emitting Diode. *Coatings* **2021**, *11*, 5. [[CrossRef](#)]
8. Prosa, M.; Benvenuti, E.; Pasini, M.; Giovanella, U.; Bolognesi, M.; Meazza, L.; Galeotti, F.; Muccini, M.; Toffanin, S. Organic Light-Emitting Transistors with Simultaneous Enhancement of Optical Power and External Quantum Efficiency via Conjugated Polar Polymer Interlayers. *ACS Appl. Mater. Interfaces* **2018**, *10*, 25580–25588. [[CrossRef](#)]
9. Boota, M.; Pasini, M.; Galeotti, F.; Porzio, W.; Zhao, M.-Q.; Halim, J.; Gogotsi, Y. Interaction of Polar and Nonpolar Polyfluorenes with Layers of Two-Dimensional Titanium Carbide (MXene): Intercalation and Pseudocapacitance. *Chem. Mater.* **2017**, *29*, 2731–2738. [[CrossRef](#)]
10. Porzio, W.; Destri, S.; Giovanella, U.; Pasini, M.; Marin, L.; Iosip, M.D.; Campione, M. Solid State Properties of Oligomers Containing Dithienothiophene or Fluorene Residues Suitable for Field Effect Transistor Devices. *Thin Solid Films* **2007**, *515*, 7318–7323. [[CrossRef](#)]
11. Giovanella, U.; Botta, C.; Galeotti, F.; Vercelli, B.; Battiato, S.; Pasini, M. Perfluorinated Polymer with Unexpectedly Efficient Deep Blue Electroluminescence for Full-Colour OLED Displays and Light Therapy Applications. *J. Mater. Chem. C* **2013**, *1*, 5322–5329. [[CrossRef](#)]
12. Giovanella, U.; Betti, P.; Bolognesi, A.; Destri, S.; Melucci, M.; Pasini, M.; Porzio, W.; Botta, C. Core-Type Polyfluorene-Based Copolymers for Low-Cost Light-Emitting Technologies. *Org. Electron.* **2010**, *11*, 2012–2018. [[CrossRef](#)]
13. Squeo, B.M.; Gasparini, N.; Ameri, T.; Palma-Cando, A.; Allard, S.; Gregoriou, V.G.; Brabec, C.J.; Scherf, U.; Chochos, C.L. Ultra Low Band Gap α,β -Unsubstituted BODIPY-Based Copolymer Synthesized by Palladium Catalyzed Cross-Coupling Polymerization for near Infrared Organic Photovoltaics. *J. Mater. Chem. A* **2015**, *3*, 16279–16286. [[CrossRef](#)]
14. Squeo, B.M.; Gregoriou, V.G.; Han, Y.; Palma-Cando, A.; Allard, S.; Serpetzoglou, E.; Konidakis, I.; Stratakis, E.; Avgeropoulos, A.; Anthopoulos, T.D.; et al. α,β -Unsubstituted Meso-Positioning Thienyl BODIPY: A Promising Electron Deficient Building Block for the Development of near Infrared (NIR) p-Type Donor–Acceptor (D–A) Conjugated Polymers. *J. Mater. Chem. C* **2018**, *6*, 4030–4040. [[CrossRef](#)]
15. Zampetti, A.; Minotto, A.; Squeo, B.M.; Gregoriou, V.G.; Allard, S.; Scherf, U.; Chochos, C.L.; Cacialli, F. Highly Efficient Solid-State Near-Infrared Organic Light-Emitting Diodes Incorporating A-D-A Dyes Based on α,β -Unsubstituted “BODIPY” Moieties. *Sci. Rep.* **2017**, *7*, 1611. [[CrossRef](#)] [[PubMed](#)]
16. Schon, T.B.; DiCarmine, P.M.; Seferos, D.S. Polyfullerene Electrodes for High Power Supercapacitors. *Adv. Energy Mater.* **2014**, *4*, 1301509. [[CrossRef](#)]
17. DiCarmine, P.M.; Schon, T.B.; McCormick, T.M.; Klein, P.P.; Seferos, D.S. Donor–Acceptor Polymers for Electrochemical Supercapacitors: Synthesis, Testing, and Theory. *J. Phys. Chem. C* **2014**, *118*, 8295–8307. [[CrossRef](#)]

18. Estrada, L.A.; Liu, D.Y.; Salazar, D.H.; Dyer, A.L.; Reynolds, J.R. Poly[Bis-EDOT-Isoindigo]: An Electroactive Polymer Applied to Electrochemical Supercapacitors. *Macromolecules* **2012**, *45*, 8211–8220. [[CrossRef](#)]
19. Wang, K.; Huang, L.; Eedugurala, N.; Zhang, S.; Sabuj, M.A.; Rai, N.; Gu, X.; Azoulay, J.D.; Ng, T.N. Wide Potential Window Supercapacitors Using Open-Shell Donor–Acceptor Conjugated Polymers with Stable N-Doped States. *Adv. Energy Mater.* **2019**, *9*, 1902806. [[CrossRef](#)]
20. McAllister, B.T.; Schon, T.B.; DiCarmine, P.M.; Seferos, D.S. A Study of Fused-Ring Thieno[3,4-e]Pyrazine Polymers as n-Type Materials for Organic Supercapacitors. *Polym. Chem.* **2017**, *8*, 5194–5202. [[CrossRef](#)]
21. van Mullekom, H.A.M.; Vekemans, J.A.J.M.; Havinga, E.E.; Meijer, E.W. Developments in the Chemistry and Band Gap Engineering of Donor–Acceptor Substituted Conjugated Polymers. *Mater. Sci. Eng. R Rep.* **2001**, *32*, 1–40. [[CrossRef](#)]
22. Aicha Youssef, A.; Mohamed Bouzzine, S.; Mohyi Eddine Fahim, Z.; Sıdır, İ.; Hamidi, M.; Bouachrine, M. Designing Donor–Acceptor Thienopyrazine Derivatives for More Efficient Organic Photovoltaic Solar Cell: A DFT Study. *Phys. B Condens. Matter* **2019**, *560*, 111–125. [[CrossRef](#)]
23. Porzio, W.; Destri, S.; Pasini, M.; Giovanella, U.; Ragazzi, M.; Scavia, G.; Kotowski, D.; Zotti, G.; Vercelli, B. Synthesis and Characterisation of Fluorenone–Thiophene-Based Donor–Acceptor Oligomers: Role of Moiety Sequence upon Packing and Electronic Properties. *New J. Chem.* **2010**, *34*, 1961–1973. [[CrossRef](#)]
24. Chochos, C.L.; Drakopoulou, S.; Katsouras, A.; Squeo, B.M.; Sprau, C.; Colsmann, A.; Gregoriou, V.G.; Cando, A.-P.; Allard, S.; Scherf, U.; et al. Beyond Donor–Acceptor (D–A) Approach: Structure–Optoelectronic Properties—Organic Photovoltaic Performance Correlation in New D–A1–D–A2 Low-Bandgap Conjugated Polymers. *Macromol. Rapid Commun.* **2017**, *38*, 1600720. [[CrossRef](#)] [[PubMed](#)]
25. Sivakumar, G.; Pratyusha, T.; Shen, W.; Gupta, D. Performance of Donor–Acceptor Copolymer Materials PCPDTBT and PCDTBT with Poly Hexyl Thiophene Polymer in a Ternary Blend. *Mater. Today Proc.* **2017**, *4*, 5060–5066. [[CrossRef](#)]
26. Zhou, H.; Yang, L.; You, W. Rational Design of High Performance Conjugated Polymers for Organic Solar Cells. *Macromolecules* **2012**, *45*, 607–632. [[CrossRef](#)]
27. Zhou, H.; Yang, L.; Price, S.C.; Knight, K.J.; You, W. Enhanced Photovoltaic Performance of Low-Bandgap Polymers with Deep LUMO Levels. *Angew. Chem. Int. Ed.* **2010**, *49*, 7992–7995. [[CrossRef](#)]
28. Shi, Z.; Ka, I.W.H.; Wang, X.; Vijila, C.; Wang, F.; Li, G.; Tjiu, W.W.; Li, J.; Xu, J. Low Band-Gap Weak Donor–Strong Acceptor Conjugated Polymer for Organic Solar Cell. *RSC Adv.* **2015**, *5*, 98876–98879. [[CrossRef](#)]
29. Zhou, H.; Yang, L.; Stoneking, S.; You, W. A Weak Donor–Strong Acceptor Strategy to Design Ideal Polymers for Organic Solar Cells. *ACS Appl. Mater. Interfaces* **2010**, *2*, 1377–1383. [[CrossRef](#)]
30. Kim, Y.J.; Kim, H.N.; Hwang, M.-C.; Kim, Y.-H.; Park, C.E. A Weak Donor/Strong Acceptor Alternating Copolymer for Efficient Bulk Heterojunction Solar Cells. *Synth. Met.* **2014**, *198*, 93–100. [[CrossRef](#)]
31. Ji, X.; Fang, L. Quinoidal Conjugated Polymers with Open-Shell Character. *Polym. Chem.* **2021**, *12*, 1347–1361. [[CrossRef](#)]
32. Huang, Y.; Egap, E. Open-Shell Organic Semiconductors: An Emerging Class of Materials with Novel Properties. *Polym. J.* **2018**, *50*, 603–614. [[CrossRef](#)]
33. Becerril, H.A.; Miyaki, N.; Tang, M.L.; Mondal, R.; Sun, Y.-S.; Mayer, A.C.; Parmer, J.E.; McGehee, M.D.; Bao, Z. Transistor and Solar Cell Performance of Donor–Acceptor Low Bandgap Copolymers Bearing an Acenaphtho[1,2-b]Thieno[3,4-e]Pyrazine (ACTP) Motif. *J. Mater. Chem.* **2009**, *19*, 591–593. [[CrossRef](#)]
34. Scharber, M.C.; Sariciftci, N.S. Low Band Gap Conjugated Semiconducting Polymers. *Adv. Mater. Technol.* **2021**, *6*, 2000857. [[CrossRef](#)]
35. Brabec, C.J.; Winder, C.; Sariciftci, N.S.; Hummelen, J.C.; Dhanabalan, A.; van Hal, P.A.; Janssen, R.A.J. A Low-Bandgap Semiconducting Polymer for Photovoltaic Devices and Infrared Emitting Diodes. *Adv. Funct. Mater.* **2002**, *12*, 709–712. [[CrossRef](#)]
36. Nie, Q.; Tang, A.; Guo, Q.; Zhou, E. Benzothiadiazole-Based Non-Fullerene Acceptors. *Nano Energy* **2021**, *87*, 106174. [[CrossRef](#)]
37. He, K.; Kumar, P.; Yuan, Y.; Li, Y. Wide Bandgap Polymer Donors for High Efficiency Non-Fullerene Acceptor Based Organic Solar Cells. *Mater. Adv.* **2021**, *2*, 115–145. [[CrossRef](#)]
38. Mondal, R.; Ko, S.; Bao, Z. Fused Aromatic Thienopyrazines: Structure, Properties and Function. *J. Mater. Chem.* **2010**, *20*, 10568–10576. [[CrossRef](#)]
39. Rasmussen, S.C.; Schwiderski, R.L.; Mulholland, M.E. Thieno[3,4-b]Pyrazines and Their Applications to Low Band Gap Organic Materials. *Chem. Commun.* **2011**, *47*, 11394–11410. [[CrossRef](#)]
40. Genene, Z.; Wang, J.; Xu, X.; Yang, R.; Mammo, W.; Wang, E. A Comparative Study of the Photovoltaic Performances of Terpolymers and Ternary Systems. *RSC Adv.* **2017**, *7*, 17959–17967. [[CrossRef](#)]
41. Kitamura, C.; Tanaka, S.; Yamashita, Y. Synthesis of New Narrow Bandgap Polymers Based on 5,7-Di(2-Thienyl)Thieno[3,4-b]Pyrazine and Its Derivatives. *J. Chem. Soc. Chem. Commun.* **1994**, *13*, 1585–1586. [[CrossRef](#)]
42. Palamà, I.; Di Maria, F.; Viola, I.; Fabiano, E.; Gigli, G.; Bettini, C.; Barbarella, G. Live-Cell-Permeant Thiophene Fluorophores and Cell-Mediated Formation of Fluorescent Fibrils. *J. Am. Chem. Soc.* **2011**, *133*, 17777–17785. [[CrossRef](#)] [[PubMed](#)]
43. Iosip, M.D.; Destri, S.; Pasini, M.; Porzio, W.; Pernstich, K.P.; Batlogg, B. New Dithieno[3,2-b:2',3'-d]Thiophene Oligomers as Promising Materials for Organic Field-Effect Transistor Applications. *Synth. Met.* **2004**, *146*, 251–257. [[CrossRef](#)]
44. Xu, B.; Pelse, I.; Agarkar, S.; Ito, S.; Zhang, J.; Yi, X.; Chujo, Y.; Marder, S.; So, F.; Reynolds, J.R. Randomly Distributed Conjugated Polymer Repeat Units for High-Efficiency Photovoltaic Materials with Enhanced Solubility and Processability. *ACS Appl. Mater. Interfaces* **2018**, *10*, 44583–44588. [[CrossRef](#)] [[PubMed](#)]

45. Schmatz, B.; Pelse, I.; Advincula, A.; Zhang, J.; Marder, S.R.; Reynolds, J.R. Photovoltaic Donor-Acceptor Conjugated Polymers with Minimally Substituted Acceptor Moieties. *Org. Electron.* **2019**, *68*, 280–284. [[CrossRef](#)]
46. Abdo, N.I.; El-Shehawey, A.A.; El-Barbary, A.A.; Lee, J.-S. Palladium-Catalyzed Direct C–H Arylation of Thieno[3,4-b]Pyrazines: Synthesis of Advanced Oligomeric and Polymeric Materials. *Eur. J. Org. Chem.* **2012**, *2012*, 5540–5551. [[CrossRef](#)]
47. Blouin, N.; Michaud, A.; Wakim, S.; Boudreault, P.-L.T.; Leclerc, M.; Vercelli, B.; Zecchin, S.; Zotti, G. Optical, Electrochemical, Magnetic, and Conductive Properties of New Polyindolocarbazoles and Polydiindolocarbazoles. *Macromol. Chem. Phys.* **2006**, *207*, 166–174. [[CrossRef](#)]
48. Reichardt, C. Solvatochromic Dyes as Solvent Polarity Indicators. *Chem. Rev.* **1994**, *94*, 2319–2358. [[CrossRef](#)]
49. Goti, G.; Calamante, M.; Coppola, C.; Dessì, A.; Franchi, D.; Mordini, A.; Sinicropi, A.; Zani, L.; Reginato, G. Donor-Acceptor-Donor Thienopyrazine-Based Dyes as NIR-Emitting AIEgens. *Eur. J. Org. Chem.* **2021**, *2021*, 2655–2664. [[CrossRef](#)]
50. Beaupré, S.; Leclerc, M. PCDTBT: En Route for Low Cost Plastic Solar Cells. *J. Mater. Chem. A* **2013**, *1*, 11097–11105. [[CrossRef](#)]
51. Scharber, M.C.; Mühlbacher, D.; Koppe, M.; Denk, P.; Waldauf, C.; Heeger, A.J.; Brabec, C.J. Design Rules for Donors in Bulk-Heterojunction Solar Cells—Towards 10% Energy-Conversion Efficiency. *Adv. Mater.* **2006**, *18*, 789–794. [[CrossRef](#)]
52. Park, S.H.; Roy, A.; Beaupré, S.; Cho, S.; Coates, N.; Moon, J.S.; Moses, D.; Leclerc, M.; Lee, K.; Heeger, A.J. Bulk Heterojunction Solar Cells with Internal Quantum Efficiency Approaching 100%. *Nat. Photon* **2009**, *3*, 297–302. [[CrossRef](#)]